



# eNRTL modelling and partition of phenolics in the ATPSs {ethyl lactate (1) + potassium sodium tartrate or disodium succinate (2) + water (3)} at 298.2 K and 0.1 MPa

Catarina S. Rebelo<sup>a,b</sup>, Pedro Velho<sup>a,b,\*</sup>, Eugenia A. Macedo<sup>a,b,\*</sup>

<sup>a</sup> LSRE-LCM – Laboratory of Separation and Reaction Engineering - Laboratory of Catalysis and Materials, Faculty of Engineering, University of Porto, Rua Dr. Roberto Frias, 4200-465 Porto, Portugal

<sup>b</sup> ALiCE – Associate Laboratory in Chemical Engineering, Faculty of Engineering, University of Porto, Rua Dr. Roberto Frias, 4200-465 Porto, Portugal

## ARTICLE INFO

### Keywords:

ATPS  
Ethyl lactate  
Antioxidants  
Ferulic acid  
Gallic acid  
eNRTL

## ABSTRACT

Ferulic (FA) and gallic (GA) acids stand as crucial antioxidants in the cosmetics, food and pharmaceutical industries, playing a key role in the prevention of diabetes, cancer and cardiovascular diseases. The extraction of these antioxidants from by-products of the food industry, such as sweet corn residues, contributes to a more circular economy, reducing the environmental footprint associated with their extraction processes.

In this work, these phenolic compounds were successfully extracted in the Aqueous Two-Phase Systems (ATPSs) {Ethyl lactate (1) + Potassium Sodium Tartrate or Disodium Succinate (2) + Water (3)} at 298.2 K and 0.1 MPa. In general, the ATPSs achieved partition coefficients ( $K$ ) larger than unity, indicating a preference towards the top phase (ethyl lactate-rich), hinting a successful extraction of the phenolic compounds. Moreover, larger tie-lines generally led to higher partition coefficients and extraction efficiencies ( $E$ ), promoting solute migration to the top phase. The most promising results referred to the partition of ferulic acid in Potassium Sodium Tartrate, with  $K = 12 \pm 3$  and  $E = 93.3 \pm 0.4\%$  for the longest tie-line (TLL = 70.73% in mass). Finally, tie-line compositions were effectively described using a generalised version of the electrolyte non-random two-liquid (eNRTL) model for double salts, presenting low standard deviations ( $\sigma_x$ ) from experimental data while considering the non-randomness factor ( $\alpha_{ij}$ ) equal to 0.2 ( $\sigma_x < 8.47 \cdot 10^{-3}$ ) and 0.3 ( $\sigma_x < 4.78 \cdot 10^{-3}$ ).

## 1. Introduction

Although Aqueous Two-Phase Systems (ATPSs) provide a sustainable alternative for the efficient recovery of biomolecules, the experimental data related to these systems is relatively scarce in literature, in particular for systems involving environmentally benign solvents, such as ethyl lactate (EL) [1–3]. ATPSs have a good scale-up potential, provide non-toxic and biocompatible extractive media and are considered eco-friendly due to their high water content [4–10]. The application of ATPSs based on organic salts, such as tartrates, succinates and citrates, has a proven lower impact on the environment than inorganic salts since the former are biodegradable and can be used as food additives [11].

Antioxidants are substances that, when present at low concentrations, delay or prevent the oxidative damage of the substrate by donating hydrogen radicals ( $H^\bullet$ ), neutralizing the reactive oxygen species (ROS) by breaking the chain of reactions and balancing their generation and

depletion [12–14]. The most abundant and widely distributed group of antioxidants are polyphenols, which play a key role in the prevention of diabetes, cancer, and neurodegenerative diseases [15,16]. Moreover, they present strong antimicrobial, anti-inflammatory and antimutagenic properties [17].

Ferulic acid ((2E) 3-(4-hydroxy-3-methoxyphenyl)prop-2-enoic acid) is a phenolic acid of low toxicity that can be found in fruits and vegetables, such as sweet corn, tomatoes, beans, oats, coffee seeds, nuts and rice bran [18]. Moreover, it is used in photoprotective cosmetic lotions given its radical scavenging capacity, which allows to suppress radiation-induced oxidative reactions, protecting cells exposed to ultraviolet (UV) radiation [18–20]. Enzymatic, alkaline or acidic extractions are often applied in the recovery of this antioxidant, but they generally fail to preserve its bioactivity, for which new approaches must be developed [21–23].

Gallic acid (3,4,5-trihydroxybenzoic acid) is a polyphenol found in

\* Corresponding authors.

E-mail addresses: [velho@fe.up.pt](mailto:velho@fe.up.pt) (P. Velho), [eamacedo@fe.up.pt](mailto:eamacedo@fe.up.pt) (E.A. Macedo).

<https://doi.org/10.1016/j.fluid.2024.114087>

Received 24 January 2024; Received in revised form 25 March 2024; Accepted 26 March 2024

Available online 31 March 2024

0378-3812/© 2024 The Authors. Published by Elsevier B.V. This is an open access article under the CC BY-NC license (<http://creativecommons.org/licenses/by-nc/4.0/>).

gallnuts, berries, grapes, mangos, hazelnuts, tea and wine, and is used in the cosmetics, pharmaceutical, leather (as chelating agent) and food (as preservative) industries [24,25]. This benzoic acid has been successfully extracted using, for example, ethanol and ionic liquids [26], and the most common methods for its quantification include ultraviolet-visible (UV-Vis) spectroscopy, chromatography, mass spectrometry and capillary electrophoresis [26,27].

During the last years, there have been numerous studies, both experimental and theoretical, on the thermodynamic properties of electrolyte solutions. Accurate thermodynamic models and process simulations of electrolyte systems are now being actively pursued to reduce the need for expensive experimental procedures, which could help the design of industrial processes aimed at the extraction of antioxidants [28–30]. For example, the recovery of electrolytes such as ferulic and gallic acids from by-products of the food sector is a promising approach to the circular economy model, and a deep knowledge on electrolyte behaviour would be advantageous for a more sustainable use of resources and to reduce the environmental impact of industrial processes [31].

Electrolyte non-random two-liquid (eNRTL) [32] is one of the most extensively applied model in the description of electrolyte-containing systems [32]. It couples the Pitzer–Debye–Hückel [33] equation for long-range ion-ion electrostatic interactions with the NRTL [34] theory, describing three types of short-range interactions: molecule-molecule, molecule-ion and ion-ion [32]. The eNRTL model is simple and capable of correctly describing the short- and long-range interactions over the entire range of concentrations and temperatures [29]. Therefore, this model provides a strong basis for reliable extrapolation, decreasing the chances of overfitting a specific data set [35]. Moreover, eNRTL can be easily extended to mixtures with multiple electrolytes and mixed solvents.

In this work, the liquid-liquid extractions of ferulic (FA) and gallic (GA) acids were performed in Aqueous Two-Phase Systems (ATPSs) of the type {ethyl lactate (1) + organic salt (2) + water (3)} at 298.2 K and 0.1 MPa, and the tie-line compositions of these systems were described using the electrolyte non-random two-liquid (eNRTL) model.

## 2. Experimental

### 2.1. Chemicals

Table 1 shows the chemicals employed in this study, along with their corresponding commercial suppliers, purities, Chemical Abstracts Service (CAS) numbers, and abbreviations. No additional pre-treatments or purification steps were undertaken.

### 2.2. Apparatus and experimental procedure

Regarding the employed apparatus, the preparation of aqueous solutions involved weighing using an ADAM AAA 250 L balance with standard measurement uncertainty of  $10^{-4}$  g. pH was assessed using a VWR pH 1100 L pH meter with standard measurement uncertainties of 0.001 and 0.1 K, and the equipment was calibrated before experimental determinations with pH standard solutions of pH = 4.00, 7.00 and 10.00 following the technical manual. Additionally, the equilibrium temperature ( $T$ ) was maintained at 298.2 K with a thermoregulated bath OvanTherm MultiMix BHM5E with a standard measurement uncertainty of 0.1 K. Liquid volume was measured with an Eppendorf Multipipette E3x electronic pipette with an uncertainty of  $2 \mu\text{L}$  (when using the 200  $\mu\text{L}$  tips) and liquid density ( $\rho$ ) was determined using an Anton Paar DSA-4500 M densimeter with standard measurement uncertainties of  $5 \cdot 10^{-5} \text{ g}\cdot\text{cm}^{-3}$  and 0.01 K. The Anton Paar DSA-4500 M densimeter was calibrated prior to use with pure water according to the technical manual. Finally, an UV-Vis Thermo Scientific Varioskan Flash spectrophotometer with standard measurement uncertainty of  $10^{-4}$  was used to

**Table 1**

- List of chemicals used and their respective suppliers, purities, CAS numbers and abbreviations.

Chemical	Supplier	Purity /% <sup>a</sup>	CAS	Abbreviation <sup>b</sup>
(-)-ethyl L-lactate (C <sub>5</sub> H <sub>10</sub> O <sub>3</sub> )	Sigma-Aldrich	> 98	97–64–3	EL
Acetic Acid (CH <sub>3</sub> COOH)	Merck	> 99	64–19–7	AcOH
Disodium succinate hexahydrate (C <sub>4</sub> H <sub>4</sub> Na <sub>2</sub> O <sub>4</sub> ·6H <sub>2</sub> O)	Tokyo Chemical Industry	> 95	6106–24–7	Na <sub>2</sub> Succinate
Ethanol (CH <sub>3</sub> CH <sub>2</sub> OH)	Sigma-Aldrich	> 99	64–17–5	EtOH
Ferulic acid (C <sub>10</sub> H <sub>10</sub> O <sub>4</sub> )	Sigma-Aldrich	> 99	537–98–4	FA
Gallic acid (C <sub>7</sub> H <sub>6</sub> O <sub>5</sub> )	Sigma-Aldrich	> 98	149–91–7	GA
Potassium sodium tartrate tetrahydrate (C <sub>4</sub> H <sub>4</sub> O <sub>6</sub> KNa·4H <sub>2</sub> O)	Sigma-Aldrich	> 99	6381–59–5	NaKTartrate
Purified water (H <sub>2</sub> O)	VWR Chemicals	–	7732–18–5	W
Sodium hydroxide (NaOH)	Merck	> 99	1310–73–2	NaOH

<sup>a</sup> Provided by the supplier in mass percentage.

<sup>b</sup> In organic salts, abbreviations refer to anhydrous moieties.

determine UV-Vis absorbance ( $A$ ), and, when needed, a VWR VV3 vortex and an IKA RO 10 P magnetic stirrer were used to stir the samples.

#### 2.2.1. Influence of pH on the UV-Vis absorbance spectrum

To minimize errors in solute quantification, it is vital to study the effect of pH on the UV-Vis absorbance spectra for the target antioxidants. Moreover, pH also affects the mean electrical charge ( $q$ ) and surface properties of these biomolecules and, consequently, their partition [4]. The mean electrical charge of these biomolecules is directly related to the  $\text{pK}_a$  values, which are linked to the release of hydrogen protons, leading to the creation of chemically distinct structures. These structures, often referred to as biomolecule or antioxidant stages, exert a significant influence on the UV-Vis absorbance spectra. Therefore, the same procedure was followed as in other works [36,37] by calculating the relative abundance of a certain acidic stage with respect to its conjugate base, following Eq. (1) [36]. This equation is only valid for very dilute antioxidant solutions.

$$\frac{[A^{q_0 \ i+1}]}{[A^{q_0 \ i}]} = 10^{\text{pH}_{\text{phase}} - \text{pK}_a^i} \quad (1)$$

where  $q_0$  represents the initial electrical charge at pH = 0,  $i$  the number of the dissociation constant ( $\text{pK}_a^i$ ) under observation,  $\text{pH}_{\text{phase}}$  the pH of the phase, and  $[A^{q_0 \ i+1}]$  and  $[A^{q_0 \ i}]$  indicate the concentrations of the antioxidant species with electrical charges of  $(q_0 \ i+1) e$  and  $(q_0 \ i) e$ , respectively.  $e$  stands for the elementary charge ( $1.602 \cdot 10^{-19} \text{ C}$ ).

Following the determination of the relative abundances for each conjugate acid-base pair, the fraction of each antioxidant species possessing an electrical charge of  $(q_0 \ i+1) e$  was calculated using Eq. (2) [36].

$$x_{A^{q_0 \ i+1}} = \frac{[A^{q_0 \ i+1}]}{[A^{q_0 \ i}]} \Bigg/ \left( \frac{[A^{q_0}]}{[A^{q_0 \ 1}]} + 1 + \sum_{j=2}^{i_{\text{max}}} \left[ \prod_{k=2}^j \frac{[A^{q_0 \ k}]}{[A^{q_0 \ (k-1)}]} \right] \right) \quad (2)$$

where  $i$  represents the number of the dissociation constant under observation and  $i_{\text{max}}$  the maximum number of protons the acid can donate.

The mean electrical charge of the antioxidant in solution ( $q$ ) was determined by applying the weighted arithmetic mean of Eq. (3) [37].

$$q = \sum_{i=1}^{i_{\max}} [x_{A^{90}} \cdot (q_0 \cdot i + 1)] + \left[ \sum_{i=1}^{i_{\max}} (x_{A^{90}} \cdot i) \right] \cdot (q_0 \cdot i_{\max}) \quad (3)$$

### 2.2.2. Partition of antioxidants

To determine the concentration of ferulic or gallic acids in a sample with unknown composition, an UV–Vis absorbance calibration curve was determined for each antioxidant. To do so, aqueous solutions with known concentrations were prepared at a pH value of approximately 7, and their UV–Vis absorbance was measured from 200 to 600 nm. Afterwards, the absorbances of the blanks (water and plate) were subtracted from the experimental data and fitted to a first-degree equation, as shown in Eq. (4).

$$A = \alpha C + \beta \quad (4)$$

where A is UV–Vis absorbance,  $\alpha$  the slope of the calibration curve, C the antioxidant concentration (in g·mL<sup>-1</sup>) and  $\beta$  is the y-intercept.

Nevertheless, it was necessary to know the phase compositions of the used ATPSS (blanks), but these were already determined in other works, for which the solubility curves and tie-line compositions were available. Hence, the partitioning of the phenolic compounds was carried out at 298.2 K and 0.1 MPa using the liquid-liquid equilibria (LLE) data from other works [38,39], as Table 2 shows.

To determine the UV–Vis absorbance of the blanks of each tie-line (TL), ternary mixtures were prepared with 10 g by pipetting pure water and ethyl lactate and aqueous solutions of the used salts (NaK-Tartrate: 33.01 % in mass; Na<sub>2</sub>Succinate: 23.83 % in mass). These mixtures were left to settle overnight (approximately 12 h) after stirring for 6 h, at 298.2 K and 0.1 MPa, and their mass, pH, UV–Vis absorbance and liquid density were measured after phase separation. In this process, triplicate measurements were conducted.

Subsequently, in the partition assays, feed compositions for the tie-lines of each ternary system were prepared with 10 g in glass vials. To maintain consistent tie-line compositions, 1 mL of water was replaced with 1 mL of aqueous solutions of ferulic acid or gallic acid (FA: 2.59·10<sup>-4</sup> g·mL<sup>-1</sup>; GA: 5.88·10<sup>-4</sup> g·mL<sup>-1</sup>). Then, vials were sealed with parafilm, capped and stirred for at least 6 h, followed by overnight settling (approximately 12 h) in a temperature-regulated bath at 298.2 K, to achieve phase equilibrium. Once again, after phase separation, the top and bottom phases were collected, and their mass, pH, UV–Vis absorbance and liquid density were measured.

Quantification of antioxidant concentrations in each phase was achieved through UV–Vis spectroscopy, leveraging the previously established calibration curves. To account for potential distortions in UV–Vis absorbance values arising from salt or ethyl lactate (EL), samples underwent analysis against their corresponding blanks. These blanks mirrored the phases of each tie-line but lacked the presence of the antioxidant under examination. Notably, interference from other sample components was found to be negligible.

To assess the separation of the top and bottom phases, the phase mass

losses ( $L_m$ ) were determined using Eq. (5).

$$L_m / \% = \frac{m_{\text{phases}}}{m_{\text{feed}}} \cdot 100 \quad (5)$$

where  $m_{\text{feed}}$  is the feed mass and  $m_{\text{phases}}$  is the sum of masses of the two separated phases.

Partition coefficients ( $K$ ), which describe the concentration ratio of the antioxidant between the two phases in equilibrium, and extraction efficiencies ( $E$ ), which refer to the percentage of antioxidant recovered in the top phase, were calculated for each tie-line using Eqs. (6) and (7), respectively [20,40].

$$K = \frac{[\text{antioxidant}]_{\text{top}}}{[\text{antioxidant}]_{\text{bot}}} \quad (6)$$

where [antioxidant] is the concentration of antioxidant in g·mL<sup>-1</sup>. The subscripts top and bot refer to the top and bottom phases, respectively.

$$E = \frac{m_{\text{top}}^{\text{antioxidant}}}{m_{\text{feed}}^{\text{antioxidant}}} \cdot 100 \quad (7)$$

where  $m_{\text{antioxidant}}$  refers to the mass of antioxidant in the indicated phase.

In Eq. (6), the antioxidant concentration is expressed in g·mL<sup>-1</sup>. Therefore, to calculate the mass of antioxidant in each phase, it is necessary to know the volume of each phase. Since both phases were weighed, the total volume of each phase can be determined using Eq. (8).

$$V_i = \frac{m_i}{\rho_i} \quad (8)$$

where  $i$  is the tie-line number,  $V$  refers to the phase volume,  $m$  to the phase mass and  $\rho$  to the liquid density.

Furthermore, to validate the obtained performance indicators ( $K$  and  $E$ ), mass balance calculations were conducted based on Eq. (9).

$$L_{s,i} = \frac{m_{s2,i} - m_{s1,i}}{m_{s1,i}} \cdot 100 \quad (9)$$

where  $L_{s,i}$  is the mass loss in quantification,  $m_{s1,i}$  refers to the mass of antioxidant present in the added 1 mL of antioxidant solution and  $m_{s2,i}$  is the quantified experimental mass of antioxidant, calculated using Eq. (10).

$$m_{s2,i} = \sum C_i^f V_i^f \quad (10)$$

where  $f$  refers to the top or bottom phase,  $C^f$  to the antioxidant concentration and  $V^f$  to the phase volume.

### 2.2.3. eNRTL modelling of tie-line data

To model tie-line compositions of the studied ATPSS, the electrolyte-Non-Random Two-Liquid (eNRTL) model was used. eNRTL takes into account the non-randomness ( $\alpha_{ij}$ ) of the interactions and assumes that

**Table 2**

- Tie-line composition, pH and tie-line length (TLL) for the ATPSS {Ethyl lactate (1) + NaKTartrate [38] or Na<sub>2</sub>Succinate [39] (2) + Water (3)}, at 298.15 K and 0.1 MPa.

No. TL	Feed			Top phase			Bottom phase			TLL /%
	$w_{\text{EL, feed}}$	$w_{\text{salt, feed}}$	$w_{\text{Water, feed}}$	$w_{\text{EL, top}}$	$w_{\text{salt, top}}$	pH	$w_{\text{EL, bot}}$	$w_{\text{salt, bot}}$	pH	
{EL (1) NaKTartrate (2) Water (3)} [38]										
1	0.320	0.130		0.538	0.042	6.62	0.137	0.200	6.61	43.10
2	0.343	0.133		0.590	0.031	6.71	0.108	0.229	6.56	52.13
3	0.365	0.137		0.637	0.023	6.64	0.082	0.255	6.56	60.15
4	0.385	0.139		0.662	0.020	6.65	0.069	0.277	6.56	64.59
5	0.414	0.142		0.700	0.016	6.61	0.054	0.305	6.56	70.73
{EL (1) Na <sub>2</sub> Succinate (2) Water (3)} [39]										
1	0.280	0.126		0.602	0.030	7.25	0.189	0.153	7.25	43.10
2	0.300	0.130		0.687	0.019	7.45	0.145	0.174	7.37	56.40
3	0.320	0.135		0.742	0.014	7.37	0.106	0.196	7.34	66.20

they can be modelled as a combination of interactions between molecules of the same type and the ones between molecules of different types [28,41]. Given that it combines the NRTL model (for short-range interactions) with the Pitzer-Debye-Hückel equation (for long-range forces), the activity coefficient of species  $i$  ( $\gamma_i$ ) is calculated using Eq. (11).

$$\ln \gamma_i = \ln \gamma_i^{\text{NRTL}} + \ln \gamma_i^{\text{PDH}} \quad (11)$$

where  $\gamma_i^{\text{NRTL}}$  and  $\gamma_i^{\text{PDH}}$  refer to the activity coefficients from the NRTL model and from the PDH equation, respectively.

The activity coefficients from the NRTL model were calculated by Eq. (12) [42].

$$\ln \gamma_i = \frac{\sum_j x_j \tau_{ji} G_{ji}}{\sum_k x_k G_{ki}} + \sum_k \frac{x_j G_{kj}}{\sum_k x_k G_{kj}} \left( \tau_{ij} \frac{\sum_l x_l \tau_{li} G_{li}}{\sum_k x_k G_{ki}} \right) \quad (12)$$

where  $\gamma_i$  is the activity coefficient of component  $i$  and  $x$  refers to the mole fraction.  $\tau_{ij}$  and  $\tau_{ji}$  are the binary interaction parameters, calculated by Eq. (13).  $G_{ij}$ ,  $G_{ji}$ ,  $G_{ki}$  and  $G_{li}$  are the excess Gibbs free energies, which are calculated by Eq. (14).

$$\tau_{ij} = \frac{g_{ij} - g_{ji}}{R_g T} \quad (13)$$

$$G_{ij} = \exp \left( \alpha_{ij} \cdot \tau_{ij} \right) \quad (14)$$

where  $g_{ij}$  and  $g_{ji}$  are the interaction energy parameters, which refer to the binary  $i-j$  and  $j-i$  interactions, and  $\alpha_{ij}$  is an adjustable parameter which describes non-randomness and is determined by fitting to experimental data (e.g., liquid-liquid equilibria data) [43,44].

The activity coefficient from the Pitzer-Debye-Hückel equation, already converted to the symmetrical convention to match the NRTL model, is given by [33]:

$$\ln \gamma_i^{\text{PDH}} = z_i^2 \cdot A_{\text{DH},x} \left[ \frac{2}{\rho} \ln \left( \frac{1 + \rho \sqrt{I_x}}{1 + \rho \sqrt{I_x^0}} \right) + \sqrt{I_x} \frac{1 - \frac{2I_x}{\rho}}{1 + \rho \sqrt{I_x}} \right] \quad (15)$$

where  $z$  is the electronic charge,  $A_{\text{DH},x}$  the Debye-Hückel parameter,  $\rho$  the closest approach parameter,  $I_x$  the ionic strength (in a mole basis) and  $I_x^0$  the ionic strength of pure electrolyte (in a mole basis).

However, Eq. (15) is not valid for salts of the types 1:2 and 2:1, known as double salts. According to Pitzer [33], in these cases,  $\gamma_i^{\text{PDH}}$  can be calculated for each cation or anion M using Eq. (16).

$$\ln \gamma_M^{\text{PDH}} = \frac{2A_{\text{DH},x}}{\sum_i x_i |z_i|} \sum_a x_a |z_a| \left\{ z_M (z_M + |z_a|) Y_{\text{Ma}} + \sum_c x_c z_c (z_c + |z_a|) \left[ \frac{z_M^2}{4I_x^{1/2}} \frac{2I_x}{1 + \rho I_x^{1/2}} \frac{z_M Y}{\sum_i x_i |z_i|} \right] \right\} \quad (16)$$

where “a” stands for the anion and “c” for the cation. M is equal to “a” in 1:2 salts and to “c” in 2:1 salts. Moreover, in the case of M being equal to “a”, the other “a” subscripts change to “c” and vice-versa. In the particular case of the electronic charges,  $z_c$  changes to  $|z_a|$  and vice-versa.

The ionic strength on a mole fraction basis ( $I_x$ ) is calculated by Eq. (17) [33].

$$I_x = \frac{\sum_c \sum_a x_c z_c x_a |z_a| (z_c + |z_a|)}{\sum_i x_i |z_i|} \quad (17)$$

In Eq. (16),  $Y$  is a function of  $\rho$  and  $I_x$ , and is calculated according to [33]:

**Table 3**

- Experimental phase mass ( $m$ ), phase mass losses ( $L_m$ ), antioxidant concentration ( $C$ ), liquid density ( $\rho$ ) and pH for the top and bottom phases in the extraction of ferulic and gallic acids in the ATPSS {Ethyl lactate (1) + NaKTartrate or Na<sub>2</sub>Succinate (2) + Water (3)}, at 298.2 K and 0.1 MPa<sup>a</sup>.

Tie-line	Phase	$m$ / g	$L_m$ / %	$C$ / g·mL <sup>-1</sup>	$\rho$ / g·mL <sup>-1</sup>	pH
Gallic acid in {EL (1) Na <sub>2</sub> Succinate (2) Water (3)}	1 Top	2.5343	0.59	7.94 · 10 <sup>-6</sup>	1.05331	7.43
	Bottom	7.4560		8.80 · 10 <sup>-5</sup>	1.13187	7.09
2 Top	2.7734	0.88	3.89 · 10 <sup>-6</sup>	1.05094	7.18	
	Bottom	7.1883		9.20 · 10 <sup>-5</sup>	1.13823	7.08
3 Top	3.3147	0.78	2.66 · 10 <sup>-6</sup>	1.04685	7.23	
	Bottom	6.7511		1.01 · 10 <sup>-4</sup>	1.14673	7.10
Ferulic acid in {EL (1) Na <sub>2</sub> Succinate (2) Water (3)}	1 Top	2.3664	0.51	6.91 · 10 <sup>-5</sup>	1.05065	7.13
	Bottom	7.6460		1.65 · 10 <sup>-5</sup>	1.12142	7.17
2 Top	2.7637	0.54	6.62 · 10 <sup>-5</sup>	1.04976	7.13	
	Bottom	7.2318		1.36 · 10 <sup>-5</sup>	1.11646	7.13
3 Top	3.3355	0.80	6.13 · 10 <sup>-5</sup>	1.04637	7.18	
	Bottom	6.6332		1.17 · 10 <sup>-5</sup>	1.14317	7.22
Gallic acid in {EL (1) NaKTartrate (2) Water (3)}	1 Top	4.5732	0.56	6.49 · 10 <sup>-5</sup>	1.10251	6.42
	Bottom	5.3971		7.16 · 10 <sup>-5</sup>	1.12078	6.62
2 Top	4.9212	0.49	6.83 · 10 <sup>-5</sup>	1.09480	6.40	
	Bottom	5.0654		6.80 · 10 <sup>-5</sup>	1.13146	6.75
3 Top	5.3427	0.39	7.12 · 10 <sup>-5</sup>	1.07553	6.71	
	Bottom	4.6558		6.42 · 10 <sup>-5</sup>	1.14649	6.95
4 Top	5.5257	0.85	7.33 · 10 <sup>-5</sup>	1.06218	6.49	
	Bottom	4.4420		6.19 · 10 <sup>-5</sup>	1.16764	7.04
5 Top	5.7553	0.60	7.55 · 10 <sup>-5</sup>	1.05683	6.84	
	Bottom	4.2334		6.04 · 10 <sup>-5</sup>	1.19553	7.06
Ferulic acid in {EL (1) NaKTartrate (2) Water (3)}	1 Top	4.8238	0.72	4.02 · 10 <sup>-5</sup>	1.06950	6.28
	Bottom	5.1533		1.87 · 10 <sup>-5</sup>	1.11754	6.77
2 Top	5.0839	0.82	4.32 · 10 <sup>-5</sup>	1.06436	6.38	
	Bottom	4.8760		1.47 · 10 <sup>-5</sup>	1.13020	6.70
3 Top	5.2756	0.79	4.60 · 10 <sup>-5</sup>	1.05445	6.47	
	Bottom	4.6844		8.75 · 10 <sup>-6</sup>	1.14582	6.85
4 Top	5.4829	0.68	4.65 · 10 <sup>-5</sup>	1.05114	6.60	
	Bottom	4.4941		6.30 · 10 <sup>-6</sup>	1.15990	6.84
5 Top	5.8762	0.67	4.54 · 10 <sup>-5</sup>	1.04784	6.70	
	Bottom	4.0933		3.84 · 10 <sup>-6</sup>	1.18348	6.86

<sup>a</sup> The standard measurement uncertainties ( $u$ ) are:  $u(m) = 1 \cdot 10^{-4}$  g,  $u(\text{pH}) = 0.001$ ,  $u(T) = 0.1$  K and  $u(\rho) = 5 \cdot 10^{-5}$  g·cm<sup>-3</sup>.

$$Y = \frac{1}{\rho} \ln \left[ \frac{1 + \rho I_x^{0.5}}{1 + \rho I_x^{0.5}} \right] \quad (18)$$

where the ionic strength of pure electrolyte ( $I_x^0$ ) is calculated using Eq. (19).

$$I_x^0 = \frac{c_a}{c_a + c_c} z_c^2 + \frac{c_c}{c_a + c_c} z_a^2 \quad (19)$$

where  $c_a$  and  $c_c$  are the stoichiometric coefficients of the anion and cation, respectively.

Besides the salt ions, two neutral species (ethyl lactate and water) exist, for which these ATPSSs constitute mixed solvent (ms) media. Therefore, some other equations were required to properly compute mixed solvent properties, which can be found in the Supplementary Materials [33,45–49].

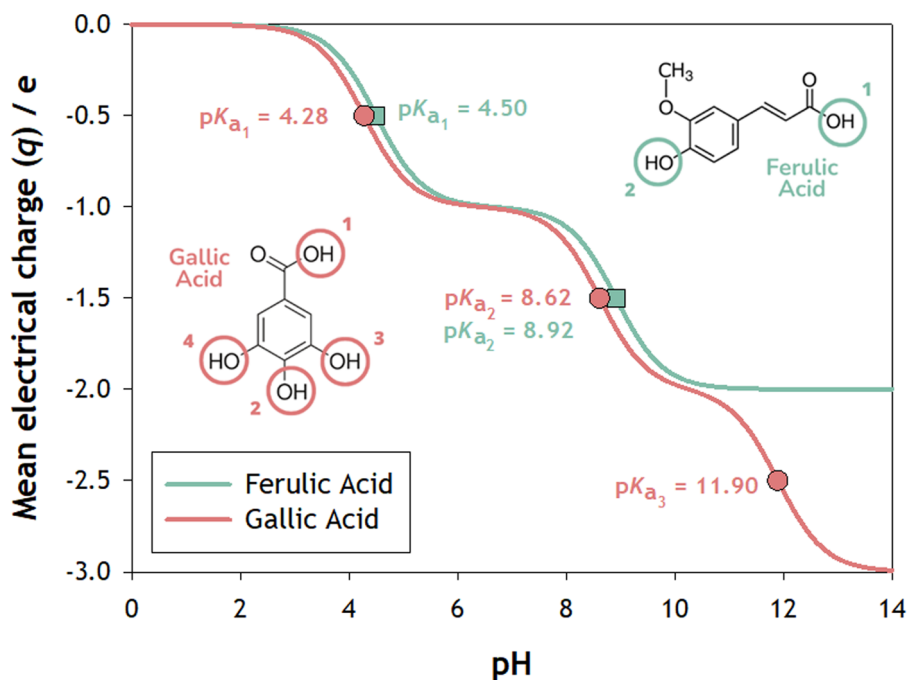


Fig. 1. - Calculated mean electrical charge ( $q$ ) for ferulic and gallic acids, expressed in terms of the elementary charge ( $e$ ), i.e.,  $1.602 \cdot 10^{-19}$  C.

### 2.3. Experimental results

All experimental results are given in Table 3.

## 3. Results and discussion

### 3.1. Influence of pH on the UV-Vis absorbance spectrum

With the reported  $pK_a$  values for ferulic (4.50 and 8.92 [50]) and gallic (4.38, 8.62, 11.90 and  $> 13$  [51,52]) acids, and using Eq. (4), the mean electrical charges ( $q$ ) of the antioxidants were calculated as a function of pH, as illustrated by Fig. 1. The calculated values of mean electrical charge and relative abundance of each antioxidant stage can be found in Tables S1 and S2, in the Supplementary Materials, for ferulic acid and gallic acid, respectively.

Both ferulic acid and gallic acid contain a carboxyl group, which is more acidic than the phenolic  $-OH$  groups, so these protons are donated first [53]. Moreover, given that the  $pK_a$  values of ferulic acid and gallic acid are similar, their mean electrical charges are alike until  $pH = 10$ . However, gallic acid presents two more phenolic groups (3 instead of 1), resulting in two additional  $pK_a$  values, i.e., in the possible donation of two more protons ( $H^+$ ). The effect of the existence of different charges due to pH differences on the UV-Vis absorbance spectra of these antioxidants was studied in the previous work [36], and their UV-Vis absorbance spectra were found to be stable at the characteristic pH of these ATPSs ( $pH \cong 7$ ), validating the chosen analytical technique.

### 3.2. Liquid-liquid extraction

Performing partition studies from real antioxidant-rich feedstock is the ultimate goal for the valorisation of biowaste and can be achieved by combining, for example, solid-liquid and liquid-liquid extraction. However, before doing so, it is vital to perform preliminary studies to find out the most promising systems for each target antioxidant (e.g., ferulic and gallic acids). After having a strong experimental background, larger scale approaches can be applied with higher success rates. Moreover, these experimental data are also very important to tune the thermodynamic models and develop more predictive approaches of solute partitioning, which could be used either to reduce the number of

experiments and to optimise the most effective ones.

To assess the potential of the studied ATPSs in the extraction of ferulic and gallic acids, feed mixtures were prepared to match the literature-based tie-line compositions and a known amount of antioxidant was added. Once equilibrium was achieved, measurements of mass, pH, density and UV-Vis absorbance were conducted, as Table 3 shows. The mass concentrations of antioxidants were then determined using UV-Vis absorbance calibration curves, which were determined at the wavelengths of 310 and 260 nm for ferulic and gallic acids, respectively. Moreover, very small losses were observed while separating the liquid phases with syringes, as shown by the low values of the phase mass losses ( $|L_m| < 0.9\%$ ), as defined by Eq. (5). These mass losses, mainly located in residues in the used vials, were found to be equally distributed by the two phases and not to change the overall compositions of the ATPSs, as shown in Table 2.

As Table 3 shows, the pH values of both phases across all systems were similar, ranging from 6.5 to 7.5, suggesting comparable distribution of antioxidant charges in both phases. Besides, the mass losses during phase separation were negligible and the higher densities observed in the bottom phases were consistent with their expected relative positions.

At the pH of the systems, which is close to 7, the chemical structures of the antioxidants in more abundance in solution are the ones presented in Fig. 2, in which both ferulic and gallic acids present a deprotonated carboxyl group, while ethyl lactate has a neutral form. Both the antioxidants have a deprotonated carboxyl group at pH close to 7, so the affinity to ethyl lactate is lower than it would be if these were in the neutral form. Comparing the two antioxidants, gallic acid is more polar because it is composed of three phenolic and one carboxylic hydroxyl groups ( $-OH$ ) capable of establishing hydrogen bonds with water, contrary to FA that only has one of each. Besides, FA has an ether group ( $OCH_3-$ ) which confers less polarity to the molecule than the phenolic groups.

As Table 3 shows, the concentration of ferulic acid in the top phases was found to lie between  $4.02 \cdot 10^{-5}$  and  $6.91 \cdot 10^{-5}$  g·mL<sup>-1</sup>, while gallic acid was quantified between  $2.66 \cdot 10^{-6}$  and  $7.55 \cdot 10^{-5}$  g·mL<sup>-1</sup>. Interestingly, even though these concentrations were limited by the useful measurement range of the UV-Vis spectrophotometer, they are still close to the ones reported for ferulic and gallic acids in, for example, aqueous

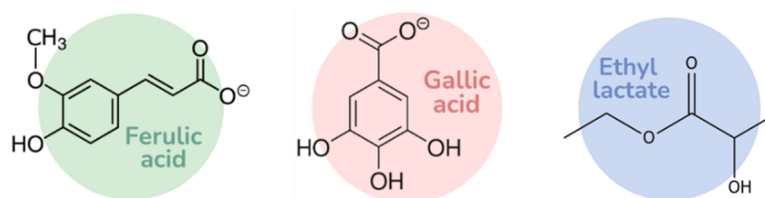


Fig. 2. - Chemical structures of ferulic acid (FA), gallic acid (GA) and ethyl lactate (EL) at the characteristic pH of the studied ATPSs ( $\text{pH} \approx 7$ ).

Table 4

- Calculated solute losses ( $L_s$ ), extraction efficiencies ( $E$ ), partition coefficients ( $K$ ) and literature-based tie-line lengths (TLL) for the extraction of ferulic and gallic acids in the ATPSs {Ethyl lactate (1) +  $\text{Na}_2\text{Succinate}$  or  $\text{NaKTartrate}$  (2) + Water (3)}, at 298.2 K and 0.1 MPa.

TL	$L_s$ / %	$E$ / %	$K$	TLL / % [38,39,55]
<b>Gallic acid in {EL (1) <math>\text{Na}_2\text{Succinate}</math> (2) Water (3)}</b>				
1	3.62	$3.182 \pm 0.004$	$0.09 \pm 0.02$	43.10
2	2.33	$2.179 \pm 0.003$	$0.05 \pm 0.02$	56.40
3	3.52	$1.352 \pm 0.002$	$0.03 \pm 0.02$	66.20
<b>Ferulic acid in {EL (1) <math>\text{Na}_2\text{Succinate}</math> (2) Water (3)}</b>				
1	1.44	$57.2 \pm 0.3$	$4.2 \pm 0.3$	43.10
2	3.52	$64.0 \pm 0.3$	$4.9 \pm 0.4$	56.40
3	3.38	$71.7 \pm 0.3$	$5.3 \pm 0.5$	66.20
<b>Gallic acid in {EL (1) <math>\text{NaKTartrate}</math> (2) Water (3)}</b>				
1	3.81	$41.74 \pm 0.06$	$0.91 \pm 0.03$	43.10
2	3.41	$48.50 \pm 0.07$	$1.00 \pm 0.04$	52.13
3	2.92	$55.88 \pm 0.08$	$1.11 \pm 0.04$	60.15
4	2.72	$60.14 \pm 0.08$	$1.18 \pm 0.04$	64.59
5	1.09	$65.06 \pm 0.09$	$1.25 \pm 0.05$	70.73
<b>Ferulic acid in {EL (1) <math>\text{NaKTartrate}</math> (2) Water (3)}</b>				
1	1.94	$66.5 \pm 0.3$	$2.2 \pm 0.2$	43.10
2	1.08	$75.7 \pm 0.3$	$2.9 \pm 0.2$	52.13
3	2.34	$84.5 \pm 0.4$	$5.3 \pm 0.6$	60.15
4	2.03	$89.0 \pm 0.4$	$7 \pm 2$	64.59
5	1.83	$93.3 \pm 0.4$	$12 \pm 3$	70.73

extracts of coffee silverskins ( $62.65 \pm 4.01$  and  $38.16 \pm 1.58 \mu\text{g} \cdot \text{g}^{-1}$  [54], respectively) and aqueous extracts of spent coffee grounds ( $65.31 \pm 5.36$  and  $53.42 \pm 4.10 \mu\text{g} \cdot \text{g}^{-1}$  [54], respectively). This means that these ATPSs could provide mass recoveries of ferulic and gallic acids close to 100 %.

Moreover, except for the partition of gallic acid in the system containing  $\text{Na}_2\text{Succinate}$ , the ATPSs presented higher antioxidant concentrations in the top phases, which suggests that the antioxidants tended to diffuse to this phase. This caused partition coefficients ( $K$ ) to be, generally, higher than unity, as shown in Table 4. The partition coefficients, determined by Eq. (10), are used to describe how a solute is

distributed between two immiscible phases, and refer to the concentration ratio, whose study is essential for the optimisation of extraction processes. Usually, the natural logarithm of the partition coefficients presents an approximately linear relation with the tie-line lengths (TLL), as Fig. 3 shows.

As Fig. 3 shows, the partitions of these antioxidants, also at 298.2 K and 0.1 MPa, in the ATPSs {Ethyl lactate (1) + trisodium citrate ( $\text{Na}_3\text{Citrate}$ ) or tripotassium citrate ( $\text{K}_3\text{Citrate}$ ) (2) + Water (3)}, conducted in a previous work [36], obtained significantly higher partition coefficients than the ones from this work. This is probably due to the presence of three carboxylate groups (deprotonated carboxyl groups) in citrate salts, which confer a more polar structure. This way, their salting-out potential is stronger, further orienting less polar molecules such as FA and GA to the least polar phase (ethyl lactate-rich, top phase).

Moreover, it was found that the partition coefficients were larger in the systems based on  $\text{NaKTartrate}$  rather than  $\text{Na}_2\text{Succinate}$ . As Fig. 4 shows,  $\text{NaKTartrate}$  presents two carboxylate groups (deprotonated carboxyl groups) and two hydroxyl groups, so it has a more polar structure than  $\text{Na}_2\text{Succinate}$ . Therefore,  $\text{NaKTartrate}$  has a stronger salting-out potential than  $\text{Na}_2\text{Succinate}$ , for which it more intensely repels less polar molecules such as ferulic acid (FA).

Concerning the extraction efficiencies ( $E$ ), as Fig. 5 shows, they generally increased with longer tie-line lengths, hinting that more distinct phase compositions promoted the migration of the solute to the top phase. Furthermore, similarly to the partition coefficients, the extraction efficiencies were larger for  $\text{Na}_3\text{Citrate}$  and  $\text{K}_3\text{Citrate}$  than  $\text{NaKTartrate}$  and  $\text{Na}_2\text{Succinate}$ , with  $\text{NaKTartrate}$  outperforming  $\text{Na}_2\text{Succinate}$ . As previously stated, this is mostly due to more polar salts more effectively repelling less polar molecules, and also explains why the partitions of gallic acid (more polar) were always less successful than the ones of ferulic acid (less polar). The most promising result obtained in this work refers to the extraction of ferulic acid in  $\text{NaKTartrate}$ , with  $K = 12 \pm 3$  and  $E = 93.3 \pm 0.4\%$  for the longest tie-line (TLL = 70.73 %), as seen in Table 4.

The analysis of the  $n$ -octanol/water partition coefficients ( $\log K_{ow}$ ) for both antioxidants aligns with these findings. This parameter measures a compound's solubility in  $n$ -octanol compared to water and serves as an

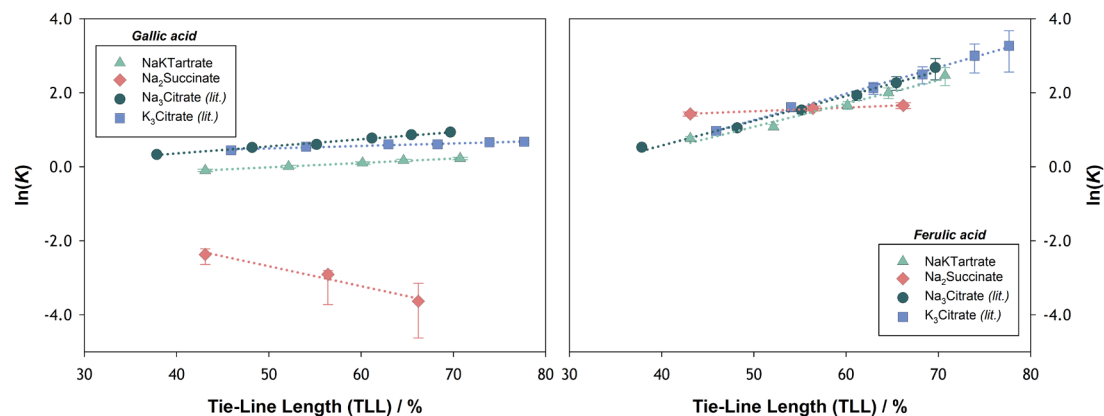


Fig. 3. - Relation between the tie-line lengths (TLL) and the natural logarithms of the experimental partition coefficients ( $K$ ) for gallic acid (left) and ferulic acid (right) in the ATPSs {Ethyl lactate (1) +  $\text{NaKTartrate}$  or  $\text{Na}_2\text{Succinate}$  or  $\text{Na}_3\text{Citrate}$  [36] or  $\text{K}_3\text{Citrate}$  [36] (2) + Water (3)}, at 298.2 K and 0.1 MPa.

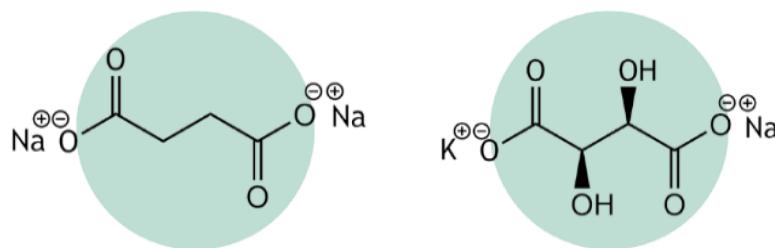


Fig. 4. - Chemical structure of the organic salts Na<sub>2</sub>Succinate (left) and NaKTartrate (right).

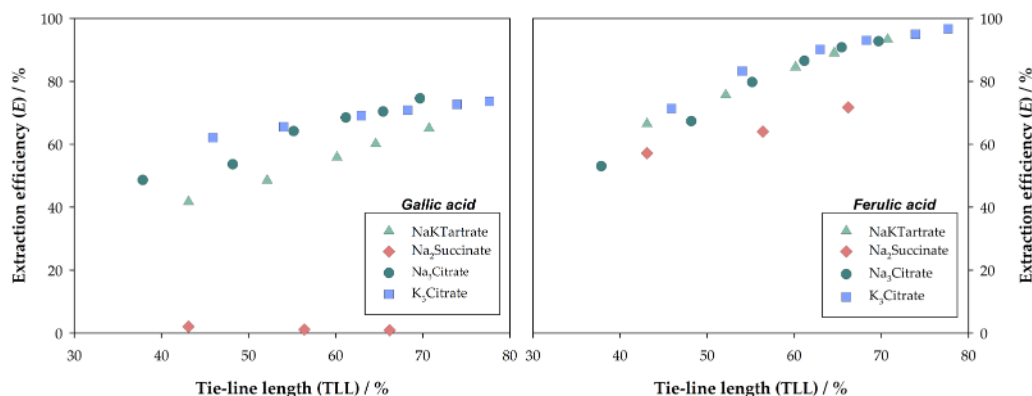


Fig. 5. - Relation between the tie-line lengths (TLL) and experimental extraction efficiencies (*E*) for gallic acid (left) and ferulic acid (right) in the ATPSs {Ethyl lactate (1) + NaKTartrate or Na<sub>2</sub>Succinate or Na<sub>3</sub>Citrate [36] or K<sub>3</sub>Citrate [36] (2) + Water (3)}, at 298.2 K and 0.1 MPa.

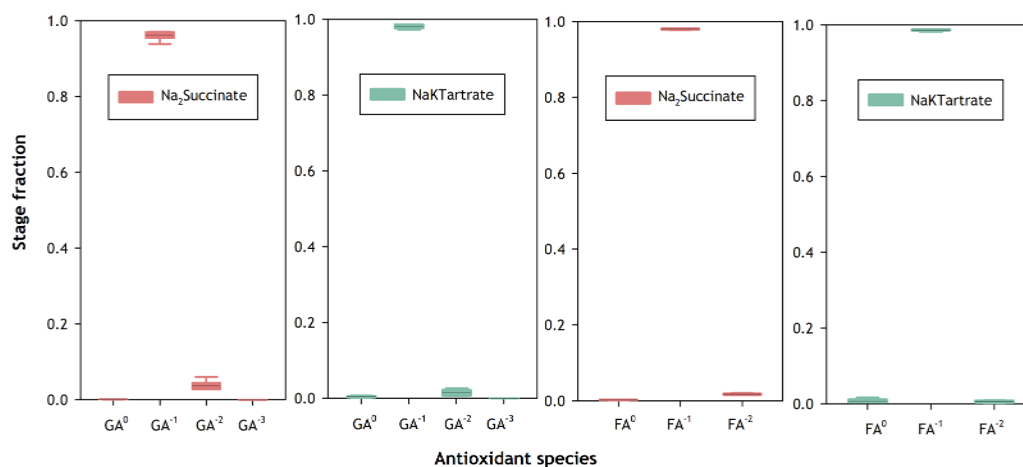


Fig. 6. - Effect of the tie-line compositions in the fractions of the antioxidant stages of gallic (GA) and ferulic (FA) acids in the ATPSs {Ethyl lactate (1) + NaKTartrate or Na<sub>2</sub>Succinate (2) + Water (3)}, at 298.2 K and 0.1 MPa. GA<sup>0</sup>, GA<sup>1</sup>, GA<sup>2</sup> and GA<sup>3</sup> refer, respectively, to the antioxidant stages of gallic acid with electrical charges equal to 0, 1, 2 and 3 e. FA<sup>0</sup>, FA<sup>1</sup> and FA<sup>2</sup> refer, respectively, to the antioxidant stages of ferulic acid with electrical charges equal to 0, 1 and 2 e.

indicator of its hydrophobicity or lipophilicity [56]. A high  $\log K_{ow}$  suggests greater solubility in octanol than water, indicating a lipophilic nature. Consequently, substances with high  $\log K_{ow}$  values tend to adsorb more readily to organic matter due to their lower affinity for water [57]. Ferulic acid and gallic acid exhibit  $\log K_{ow}$  values of 1.58 [58] and 0.89 [59], respectively, for which FA has a higher affinity for phases with lower water content, as verified in this work.

Moreover, distinct pH values were obtained depending on tie-line composition. Consequently, the distribution of antioxidant stages may not be equal in all tie-lines, so it is crucial to assess their distribution. As Fig. 6 shows, similar distributions of the studied antioxidants were observed across the tested ATPSs. Since gallic acid is more reactive (chemically unstable), small variances in the pH resulted in disparities in

the fraction of the antioxidant stages. This antioxidant was significantly more affected since it has a  $pK_a$  near the systems' pH. For ferulic acid, it was concluded that the tested tie-line compositions yielded the same distribution of electrical charges.

Given its superior stability and larger performance indicators (partition coefficients and extraction efficiencies), particularly to what concerns the {EL (1) + NaKTartrate (2) + Water (3)} system, the recovery of ferulic acid in the studied ATPSs was considered more promising than the one of gallic acid. Moreover, the tested ATPSs are either based on NaKTartrate or Na<sub>3</sub>Citrate, which are considered non-toxic organic salts with wide application in the food industry (NaKTartrate: production of pectins and jellies; Na<sub>3</sub>Citrate: buffering and emulsifying agent). Therefore, these salting out agents could be microencapsulated

together with the extracted antioxidants and used as, for example, food supplements. On the other hand, if the antioxidants are directly extracted from bio residues, the environmental footprint of these processes could be decreased, and a more circular economy would be promoted.

### 3.3. eNRTL modelling of tie-line data

In the thermodynamic modelling of the tie-line compositions of the ATPSs {Ethyl lactate (1) + NaKTartrate [38] or Na<sub>2</sub>Succinate [39] or Na<sub>3</sub>Citrate [55] or K<sub>3</sub>Citrate [55] (2) + Water (3)}, organic salts were considered as strong salts (fully dissociated), for which a specific term had to be used to account for long-range interactions (caused by the existence of charged species). Therefore, two solvents (ethyl lactate and water) and two ions (salt-cation and salt-anion) were considered in the modelled ATPSs, apart from the system containing NaKTartrate, which contains three ions (two salt-cations and one salt-anion). The existence of this double salt required the generalisation of the eNRTL model, as seen in Eqs. (16) to (19), and the consideration of a mixed solvent (ms) by the application of equations (S1) to (S9), in the Supplementary Materials.

In the electrolyte non-random two-liquid (eNRTL) [32] model, short-range electrostatic interactions between ions and solvents are described by the NRTL model, while the long-range electrostatic forces, which are dominant, are represented by the Pitzer-Debye-Hückel equation (PDH) [28,60]. Nevertheless, eNRTL is based on the same assumptions as the NRTL [34] model, which considers that the non-ideality of the mixture arises from the differences in the molecular size, shapes, and polarity of the components.

To conduct the thermodynamic modelling, an algorithm was developed in this work. In each system, two different values of the non-randomness parameter ( $\alpha_{ij} = 0.2$  and  $0.3$ ) were tested to evaluate the best approach, and the binary interaction parameters ( $\tau_{ij}$ ) were optimised until the standard deviation to experimental data ( $\sigma_x$ ) was minimised and the isoactivity criterion (IC) was achieved. Moreover, the van der Waals volume ( $V_w$ ) of each species was calculated following the Bondi's group contribution method [48] and can be found in Table S3, in the Supplementary Materials. The obtained parameters in the modelling of the studied ATPSs, together with the respective standard deviations, can be observed in Tables S4-S7, in the Supplementary Materials.

As Fig. 7 shows, most systems presented better results when considering  $\alpha_{ij} = 0.3$ , for which modelling accuracy was generally favoured by considering larger non-randomness factors, *i.e.*, more defined

spatial orientations of the molecules (higher polarity). The only exception is trisodium citrate (Na<sub>3</sub>Citrate), in which  $\alpha_{ij} = 0.2$  achieved significantly better results ( $\sigma_x = 1.57 \cdot 10^{-3}$ ) than  $\alpha_{ij} = 0.3$  ( $\sigma_x = 4.78 \cdot 10^{-3}$ ). Even though it is risky to attribute a specific physical justification to this exception, trisodium citrate is known to present stronger ion pairing than tripotassium citrate, for which dipoles become less intense in the former salt. Consequently, its spatial distribution is more random and its non-randomness factor is closer to zero [44].

Furthermore, considering the obtained values of standard deviations ( $\sigma_x < 8.47 \cdot 10^{-3}$ ), as shown in Tables S4-S7, in the Supplementary Materials, it can be concluded that the modelling results were in good agreement with the liquid-liquid equilibria data. Therefore, the eNRTL model accurately predicted the phase diagrams of the studied ATPSs and an almost complete overlap between the experimental and the modelling data was achieved, for example, for the ATPS containing NaKTartrate. In Fig. 8, the best modelling results for each system are shown and compared with the respective experimental liquid-liquid equilibria data.

## 4. Conclusions

The primary purpose of this work was to study the efficiency of extraction of ferulic (FA) and gallic (GA) acids in green Aqueous Two-Phase Systems (ATPSs) containing ethyl lactate, water and an organic salt (disodium succinate or potassium sodium tartrate), at 298.2 K and 0.1 MPa. In general, the studied ATPSs exhibited partition coefficients ( $K$ ) higher than unity, indicating a propensity for antioxidants to diffuse into the ethyl lactate-rich phase (top phase). This observation suggests the success of ATPSs in extracting these species, and the obtained results revealed that larger tie-lines generally promoted higher performance indicators, favouring the migration of solutes to the top phase. The largest values of these parameters were obtained for ferulic acid in NaKTartrate ( $K = 12 \pm 3$  and  $E = 93.3 \pm 0.4\%$ ) for the longest tie-line (TLL = 70.73%). Additionally, the studied ternary systems were satisfactorily described using a generalised version of the electrolyte non-random two-liquid (eNRTL) model for double salts. This approach consists of the NRTL model coupled with the Pitzer-Debye-Hückel (PDH) equation and successfully predicted the behaviour of the studied ATPSs, obtaining low standard deviations ( $\sigma_x < 8.47 \cdot 10^{-3}$ ) from experimental liquid-liquid equilibria data.

Hence, the studied ATPSs provided promising alternatives for the separation of ferulic and gallic acids, which could accelerate a more sustainable valorisation of agricultural by-products, contributing to a

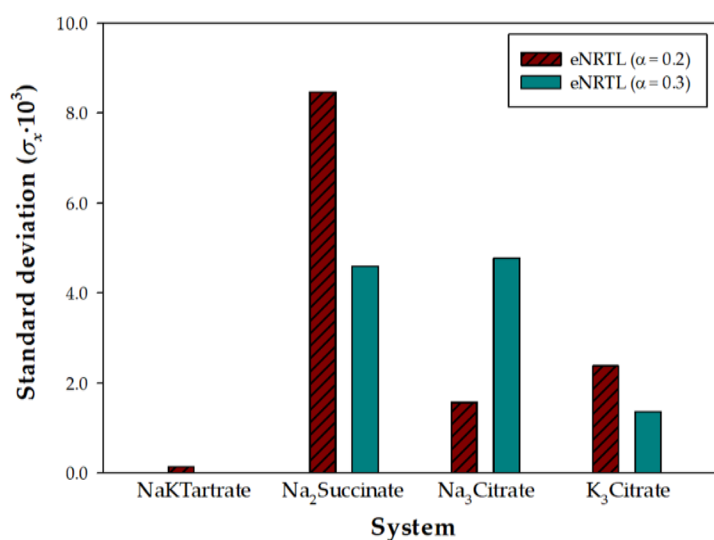
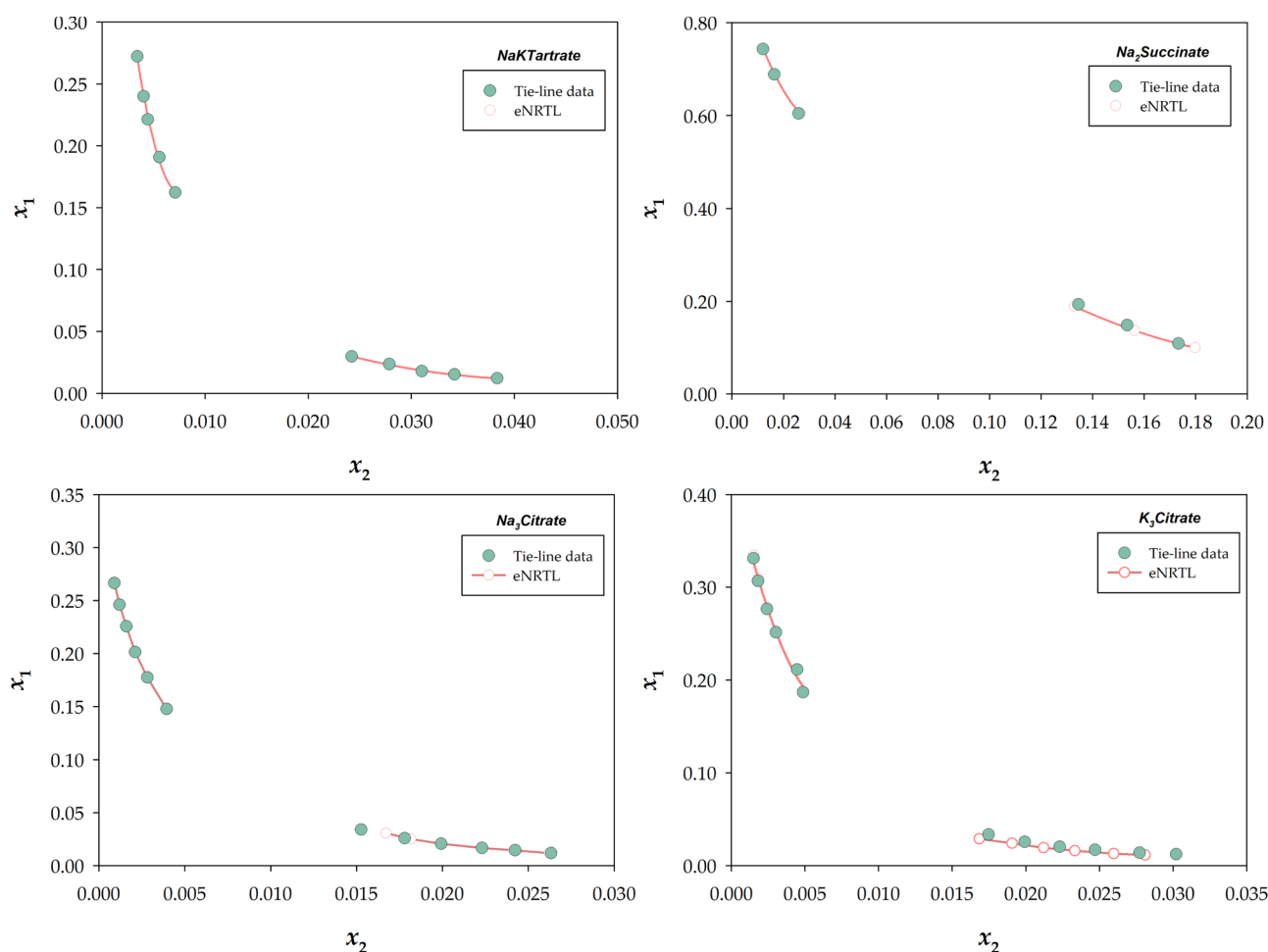


Fig. 7. - Standard deviations ( $\sigma_x$ ) from experimental data obtained in the modelling of the tie-line compositions of the ATPSs {Ethyl lactate (1) + NaKTartrate or Na<sub>2</sub>Succinate or Na<sub>3</sub>Citrate or K<sub>3</sub>Citrate (2) + Water (3)}, at 298.2 K and 0.1 MPa, using eNRTL.



**Fig. 8.** - Experimental tie-line composition data, at 298.2 K and 0.1 MPa, for the ATPS {Ethyl lactate (1) + NaKTartrate or Na<sub>2</sub>Succinate or Na<sub>3</sub>Citrate or K<sub>3</sub>Citrate (2) + Water (3)}, and respective prediction using eNRTL. Only the best approach ( $\alpha = 0.2$  or  $\alpha = 0.3$ ) is shown for each system.

more circular economy. Moreover, the application of the eNRTL model to the liquid-liquid equilibria data of these systems could help develop more predictive methodologies.

#### CRediT authorship contribution statement

**Catarina S. Rebelo:** Writing – review & editing, Writing – original draft, Visualization, Investigation, Formal analysis. **Pedro Velho:** Writing – review & editing, Writing – original draft, Methodology, Investigation, Formal analysis, Conceptualization. **Eugenia A. Macedo:** Writing – review & editing, Supervision, Conceptualization.

#### Declaration of competing interest

The authors declare that they have no known competing financial interests or personal relationships that could have appeared to influence the work reported in this paper.

#### Data availability

Data will be made available on request.

#### Acknowledgements

This work was supported by national funds through FCT/MCTES (PIDDAC): LSRE-LCM, UIDB/50020/2020 (DOI: 10.54499/UIDB/

50020/2020) and UIDP/50020/2020 (DOI: 10.54499/UIDP/50020/2020); and ALiCE, LA/P/0045/2020 (DOI: 10.54499/LA/P/0045/2020). Catarina S. Rebelo acknowledges funding from Project 2SMART – Engineered Smart Materials for Smart Citizens (NORTE-01-0145-FEDER-000054), supported by Norte Portugal Regional Operational Programme (NORTE 2020), under the PORTUGAL 2020 Partnership Agreement, through the European Regional Development Fund (ERDF). Pedro Velho is grateful for the funding support from FCT, Portugal [2021.06626.BD].

#### Supplementary Materials

In the Supplementary Materials, the equations used to describe the properties of the mixed solvent in the eNRTL model are shown, together with the obtained parameters and standard deviations ( $\sigma_x$ ) from experimental data. Moreover, the calculated mean electrical charges ( $q$ ) of the antioxidants at different pH values are presented.

#### Supplementary materials

Supplementary material associated with this article can be found, in the online version, at [doi:10.1016/j.fluid.2024.114087](https://doi.org/10.1016/j.fluid.2024.114087).

#### References

- [1] F.H.B. Sosa, F.O. Farias, L. Igarashi-Mafra, M.R. Mafra, Measurement and correlation of aqueous two-phase systems of polyvinylpyrrolidone (PVP) and

- manganese sulfate: effects of molecular weight and temperature, *Fluid Phase Equilib.* 472 (2018) 204–211, <https://doi.org/10.1016/j.fluid.2018.05.021>.
- [2] N. Ferricheva, L. Ninni, G. Maurer, Aqueous two-phase systems of poly(vinyl pyrrolidone) and sodium sulfate: experimental results and correlation/prediction, *J. Chem. Eng. Data* 52 (2007), <https://doi.org/10.1021/je7002012>.
- [3] P. Velho, L. Marques, E.A. Macedo, Extraction of polyphenols and vitamins using biodegradable ATPS based on ethyl lactate, *Molecules* 27 (2022) 7838, <https://doi.org/10.3390/molecules27227838>.
- [4] M. Iqbal, Y. Tao, S. Xie, Y. Zhu, D. Chen, X. Wang, L. Huang, D. Peng, A. Sattar, M. A.B. Shabbir, H.I. Hussain, S. Ahmed, Z. Yuan, Aqueous two-phase system (ATPS): an overview and advances in its applications, *Biol. Proced. Online* 18 (2016) 18, <https://doi.org/10.1186/s12575-016-0048-8>.
- [5] A.R. Titus, P.P. Madeira, L.A. Ferreira, V.Y. Chernyak, V.N. Uversky, B. Y. Zaslavsky, Mechanism of phase separation in aqueous two-phase systems, *Int. J. Mol. Sci.* 23 (2022), <https://doi.org/10.3390/ijms232214366>.
- [6] J. Benavides, M. Rito-Palomares, J.A. Asenjo, Aqueous two-phase systems, Academic Press (2011), <https://doi.org/10.1016/B978-0-08-088504-9.00124-0>.
- [7] M. Gonzalez-Amado, O. Rodríguez, A. Soto, P. Carbonell-Hermida, M.d.M. Olaya, A. Marcilla, Aqueous two-phase systems: a correlation analysis, *Ind. Eng. Chem. Res.* 59 (2020) 6318–6328, <https://doi.org/10.1021/acs.iecr.9b06078>.
- [8] D.R. Baughman, Y.A. Liu, Development of expert networks: a hybrid system of expert systems and neural networks, Academic Press (1995), <https://doi.org/10.1016/B978-0-12-083030-5.50012-6>.
- [9] Y.K. Yau, C.W. Ooi, E.-P. Ng, J.C.-W. Lan, T.C. Ling, P.L. Show, Current applications of different type of aqueous two-phase systems, *BIOB* 2 (2015) 49, <https://doi.org/10.1186/s40643-015-0078-0>.
- [10] Y. Chao, H.C. Shum, Emerging aqueous two-phase systems: from fundamentals of interfaces to biomedical applications, *Chem. Soc. Rev.* 49 (2019) 114–142, <https://doi.org/10.1039/C9CS00466A>.
- [11] M.T. Zafarani-Moattar, P. Seifi-Aghjekohal, Liquid–liquid equilibria of aqueous two-phase systems containing polyvinylpyrrolidone and tripotassium phosphate or dipotassium hydrogen phosphate: experimental and correlation, *Calphad* 31 (2007) 553–559, <https://doi.org/10.1016/j.calphad.2007.02.001>.
- [12] A.M. Pisoschi, A. Pop, The role of antioxidants in the chemistry of oxidative stress: a review, *Eur. J. Med. Chem.* 97 (2015) 55–74, <https://doi.org/10.1016/j.ejmech.2015.04.040>.
- [13] B. Poljsak, D. Suput, I. Milisav, Achieving the balance between ROS and antioxidants: when to use the synthetic antioxidants, *Oxid. Med. Cell. Longevity* 2013 (2013) 956792, <https://doi.org/10.1155/2013/956792>.
- [14] J. Bouayed, T. Bohn, Exogenous antioxidants - double-edged swords in cellular redox state: health beneficial effects at physiologic doses versus deleterious effects at high doses, *Oxid. Med. Cell. Longevity* 3 (2010) 228–237, <https://doi.org/10.4161/oxim.3.4.12858>.
- [15] A. Scalbert, I.T. Johnson, M. Saltmarsh, Polyphenols: antioxidants and beyond, *Am. J. Clin. Nutr.* 81 (2005), <https://doi.org/10.1093/ajcn/81.1.215S>.
- [16] M. Abbas, F. Saeed, F.M. Anjum, M. Afzaal, T. Tufail, M.S. Bashir, A. Ishtiaq, S. Hussain, H.A.R. Suleria, Natural polyphenols: an overview, *Int. J. Food Prop.* 20 (2017) 1689–1699, <https://doi.org/10.1080/10942912.2016.1220393>.
- [17] A. Cencic, W. Chingwaru, The role of functional foods, nutraceuticals, and food supplements in intestinal health, *Nutrients* 2 (2010) 611–625.
- [18] E. Graf, Antioxidant potential of ferulic acid, *free radic.*, *Biol. Med.* 13 (1992) 435–448, [https://doi.org/10.1016/0891-5849\(92\)90184-1](https://doi.org/10.1016/0891-5849(92)90184-1).
- [19] S. Ou, K.-C. Kwok, Ferulic acid: pharmaceutical functions, preparation and applications in foods, *J. Sci. Food Agric.* 84 (2004) 1261–1269, <https://doi.org/10.1002/jsfa.1873>.
- [20] N. Kumar, V. Pruthi, Potential applications of ferulic acid from natural sources, *Biotechnol. Rep.* 4 (2014) 86–93, <https://doi.org/10.1016/j.btre.2014.09.002>.
- [21] A. Tilay, M. Bule, J. Kishenkumar, U. Annapure, Preparation of ferulic acid from agricultural wastes: its improved extraction and purification, *J. Agric. Food Chem.* 56 (2008) 7644–7648, <https://doi.org/10.1021/jf801536t>.
- [22] C. Conidi, L. Donato, C. Algieri, A. Cassano, Valorization of chestnut processing by-products: a membrane-assisted green strategy for purifying valuable compounds from shells, *J. Clean. Prod.* 378 (2022) 134564, <https://doi.org/10.1016/j.jclepro.2022.134564>.
- [23] F. Caponio, A. Piga, M. Poiana, Valorization of food processing by-products, *Foods* 11 (2022) 3246, <https://doi.org/10.3390/foods11203246>.
- [24] W. Bors, C. Michel, Chemistry of the antioxidant effect of polyphenols, *Ann. N. Y. Acad. Sci.* 957 (2002) 57–69, <https://doi.org/10.1111/j.1749-6632.2002.tb02905.x>.
- [25] C. Tsiptsias, I. Tsvintzelis, Insights on thermodynamic thermal properties and infrared spectroscopic band assignments of gallic acid, *J. Pharm. Biomed. Anal.* 221 (2022) 115065, <https://doi.org/10.1016/j.jpba.2022.115065>.
- [26] Y.Y. Ow, I. Stupans, Gallic acid and gallic acid derivatives: effects on drug metabolizing enzymes, *Curr. Drug Metab.* 4 (2003) 241–248, <https://doi.org/10.2174/1389200033489479>.
- [27] F.H.A. Fernandes, H.R.N. Salgado, Gallic Acid: review of the methods of determination and quantification, *Crit. Rev. Anal. Chem.* 46 (2016) 257–265, <https://doi.org/10.1080/10408347.2015.1095064>.
- [28] G.M. Kontogeorgis, G.K. Folas, Thermodynamic models for industrial applications: from classical and advanced mixing rules to association theories, Wiley (2009), <https://doi.org/10.1002/9780470747537>.
- [29] N. Boukhalfa, A.-H. Meniai, Thermodynamic modeling of aqueous electrolytes type 2-1, *Procedia Eng.* 148 (2016) 1121–1129, <https://doi.org/10.1016/j.proeng.2016.06.560>.
- [30] C. Christov, Thermodynamics of formation of double salts and mixed crystals from aqueous solutions, *J. Chem. Thermodyn.* 37 (2005) 1036–1060, <https://doi.org/10.1016/j.jct.2005.01.008>.
- [31] F. Fernandes, K. Gorissen, C. Delerue-Matos, C. Grosso, Valorisation of agro-food by-products for the extraction of phenolic compounds, *Biol. Life Sci. Forum* 18 (2022) 61, <https://doi.org/10.3390/Foods2022-13032>.
- [32] C.-C. Chen, Y. Song, Generalized electrolyte-NRTL model for mixed-solvent electrolyte systems, *AIChE J.* 50 (2004) 1928–1941, <https://doi.org/10.1002/aic.10151>.
- [33] K.S. Pitzer, Activity coefficients in electrolyte solutions, CRC Press (1991), <https://doi.org/10.1201/9781351069472>.
- [34] H. Renon, J.M. Prausnitz, Local compositions in thermodynamic excess functions for liquid mixtures, *AIChE J.* 14 (1968) 135–144, <https://doi.org/10.1002/aic.690140124>.
- [35] C.-C. Chen, H.I. Britt, J.F. Boston, L.B. Evans, Local composition model for excess Gibbs energy of electrolyte systems. Part I: single solvent, single completely dissociated electrolyte systems, *AIChE J.* 28 (1982) 588–596, <https://doi.org/10.1002/aic.690280410>.
- [36] P. Velho, C.S. Rebelo, E.A. Macedo, Extraction of gallic acid and ferulic acid for application in hair supplements, *Molecules* 28 (2023) 2369, <https://doi.org/10.3390/molecules28052369>.
- [37] C.S. Rebelo, P. Velho, E.A. Macedo, Partition studies of resveratrol in low-impact ATPS for food supplementation, *Ind. Eng. Chem. Res.* (2024), <https://doi.org/10.1021/acs.iecr.3c03969>.
- [38] P.F. Requejo, P. Velho, E. Gomez, E.A. Macedo, Study of liquid–liquid equilibrium of aqueous two-phase systems based on ethyl lactate and partitioning of Rutin and Quercetin, *Ind. Eng. Chem. Res.* 59 (2020) 21196–21204, <https://doi.org/10.1021/acs.iecr.0c02664>.
- [39] I. Kamalanathan, Z. Petrovski, L.C. Branco, V. Najdanovic-Visak, Novel aqueous biphasic system based on ethyl lactate for sustainable separations: phase splitting mechanism, *J. Mol. Liq.* 262 (2018) 37–45, <https://doi.org/10.1016/j.molliq.2018.03.119>.
- [40] L. Fremont, Biological effects of resveratrol, *Life Sci.* 66 (2000) 663–673, [https://doi.org/10.1016/S0024-3205\(99\)00410-5](https://doi.org/10.1016/S0024-3205(99)00410-5).
- [41] M.J. Assael, J.P.M. Trusler, T.F. Tsolakis, Activity coefficient models, in, *Thermophys. Prop. Fluids* (1996) 161–206, [https://doi.org/10.1142/9781848161054\\_0007](https://doi.org/10.1142/9781848161054_0007).
- [42] Y. Dadmohammadi, S. Gebreyohannes, B.J. Neely, K.A.M. Gasem, Multicomponent phase behavior predictions using QSPR-generalized NRTL and UNIQUAC models, *Fluid Phase Equilib.* 409 (2016) 318–326, <https://doi.org/10.1016/j.fluid.2015.10.009>.
- [43] I.D.G. Chaves, J.R.G. Lopez, J.L.G. Zapata, A.L. Robayo, G.R. Niño, Thermodynamic and property models, in: *Process Analysis and Simulation in Chemical Engineering*, Springer International Publishing, Cham, 2016, pp. 53–102, [https://doi.org/10.1007/978-3-319-14812-0\\_2](https://doi.org/10.1007/978-3-319-14812-0_2).
- [44] P. Velho, L.R. Barroca, E.A. Macedo, A geometric approach for the calculation of the nonrandomness factor using computational chemistry, *J. Chem. Eng. Data* (2023), <https://doi.org/10.1021/acs.jced.3c00532>.
- [45] K.S. Pitzer, J.M. Simonson, Thermodynamics of multicomponent, miscible, ionic systems: theory and equations, *J. Phys. Chem.* 90 (1986) 3005–3009, <https://doi.org/10.1021/j100404a042>.
- [46] P. Velho, E. Gomez, E.A. Macedo, Calculating the closest approach parameter for ethyl lactate-based ATPS, *Fluid Phase Equilib.* 556 (2022) 113389, <https://doi.org/10.1016/j.fluid.2022.113389>.
- [47] G. Oster, The Dielectric properties of liquid mixtures, *J. Am. Chem. Soc.* 68 (1946) 2036–2041, <https://doi.org/10.1021/ja01214a050>.
- [48] A. Bondi, van der waals volumes and radii, *J. Phys. Chem.* 68 (1964) 441–451, <https://doi.org/10.1021/j100785a001>.
- [49] P. Velho, C. Lopes, E.A. Macedo, Predicting the ionicity of ionic liquids in binary mixtures based on solubility data: II, *Fluid Phase Equilib.* 569 (2023) 113766, <https://doi.org/10.1016/j.fluid.2023.113766>.
- [50] F. Borges, J.L.F.C. Lima, I. Pinto, S. Reis, C. Siquet, Application of a potentiometric system with data-analysis computer programs to the quantification of metal-chelating activity of two natural antioxidants: caffeic acid and ferulic acid, *Helv. Chim. Acta* 86 (2003) 3081–3087, <https://doi.org/10.1002/hlca.200390250>.
- [51] D.W. Fink, J.D. Stong, The electronic spectral properties of gallic acid, *Spectrochim. Acta, Part A* 38 (1982) 1295–1298, [https://doi.org/10.1016/0584-8539\(82\)80127-X](https://doi.org/10.1016/0584-8539(82)80127-X).
- [52] A.C. Eslami, W. Pasanphan, B.A. Wagner, G.R. Buettner, Free radicals produced by the oxidation of gallic acid: an electron paramagnetic resonance study, *Chem. Cent. J.* 4 (2010) 15, <https://doi.org/10.1186/1752-153X-4-15>.
- [53] N.A. Ramaiah, R.K. Chaturvedi, Potentiometric studies on the dissociation of gallic acid, *Proc. Indian Acad. Sci.* 51 (1960) 177–188, <https://doi.org/10.1007/BF03045780>.
- [54] G. Zengin, K.I. Sinan, M.F. Mahomoodally, S. Angeloni, A.M. Mustafa, S. Vittori, F. Maggi, G. Caprioli, Chemical composition, antioxidant and enzyme inhibitory properties of different extracts obtained from spent coffee ground and coffee silverskin, *Foods* 9 (2020) 713, <https://doi.org/10.3390/foods9060713>.
- [55] P. Velho, P.F. Requejo, E. Gomez, E.A. Macedo, Novel ethyl lactate based ATPS for the purification of rutin and quercetin, *Sep. Purif. Technol.* 252 (2020) 117447, <https://doi.org/10.1016/j.seppur.2020.117447>.
- [56] A. Sridhar, M. Ponnuchamy, P.S. Kumar, A. Kapoor, D.N. Vo, S. Prabhakar, Techniques and modeling of polyphenol extraction from food: a review, *Environ. Chem. Lett.* 19 (2021) 3409–3443, <https://doi.org/10.1007/s10311-021-01217-8>.

- [57] M.M. Miller, S.P. Wasik, G.L. Huang, W.Y. Shiu, D. Mackay, Relationships between octanol-water partition coefficient and aqueous solubility, *Environ. Sci. Technol.* 19 (1985) 522–529, <https://doi.org/10.1021/es00136a007>.
- [58] N.D. Raj, D. Singh, A critical appraisal on ferulic acid: biological profile, biopharmaceutical challenges and nano formulations, *Health Sci. J.* 5 (2022) 100063, <https://doi.org/10.1016/j.hsr.2022.100063>.
- [59] C. Locatelli, R. Rosso, M.C. Santos-Silva, C. Souza, M. Licínio, P. Leal, M.L. Bazzo, R. Yunes, T. Creczynski-Pasa, Ester derivatives of gallic acid with potential toxicity toward L1210 leukemia cells, *Bioorg. Med. Chem.* 16 (2008) 3791–3799, <https://doi.org/10.1016/j.bmc.2008.01.049>.
- [60] C.-K. Chang, S.-T. Lin, Extended pitzer–debye–hückel model for long-range interactions in ionic liquids, *J. Chem. Eng. Data* 65 (2020) 1019–1027, <https://doi.org/10.1021/acs.jced.9b00368>.